

UniPLV: Towards Label-Efficient Open-World 3D Scene Understanding by Regional Visual Language Supervision

Yuru Wang, Songtao Wang, Zehan Zhang*, Xinyan Lu, Changwei Cai, Hao Li,
Fu Liu, Peng Jia, and Xianpeng Lang
Li Auto Inc.

wangyurul@lixiang.com; zhangzehan@lixiang.com

Abstract

We present *UniPLV*, a powerful framework that unifies point clouds, images and text in a single learning paradigm for open-world 3D scene understanding. *UniPLV* employs the image modal as a bridge to co-embed 3D points with pre-aligned images and text in a shared feature space without requiring carefully crafted point cloud text pairs. To accomplish multi-modal alignment, we propose two key strategies: (i) logit and feature distillation modules between images and point clouds, and (ii) a vision-point matching module is given to explicitly correct the misalignment caused by points to pixels projection. To further improve the performance of our unified framework, we adopt four task-specific losses and a two-stage training strategy. Extensive experiments show that our method outperforms the state-of-the-art methods by an average of 15.6% and 14.8% for semantic segmentation over Base-Annotated and Annotation-Free tasks, respectively. The code will be released later.

1. Introduction

Open-world 3D scene understanding aims to obtain a model that can distinguish and recognize open-set objects and categories from 3D data, e.g. point clouds, without manual annotations. Traditional closed-set 3D understanding relying on manual annotations cannot accomplish the task of open-set recognition. Therefore, open-world 3D scene understanding is critical for real-world applications, such as autonomous driving, mobile robots, virtual reality, etc.

Recent success of visual language models (VLM) has provided opportunities for open-world 3D scene understanding. Frozen-VLM labeling-based methods [22, 38] transfer the open vocabulary of VLM to 3D scenes for implementing open-world 3D scene understanding. These methods neglect region-level feature distillation learning and require resource-intensive feature extraction, fusion,

and storage processes [40], thus hindering scalability to more advanced 3D networks and 3D scenes, which in turn makes it difficult to improve performance. Pairs-construction based methods [7, 8, 33] attempts to align point clouds and text like VLM training by constructing point clouds text pairs. RegionPLC [33] achieves the state-of-the-art (SOTA) performance, but requires a tedious process to produce a large number of point clouds text pairs for contrastive training. However, unlike VLM that can obtain large-scale text-image pairs from the Internet, point cloud text pairs cannot be easily obtained, resulting in performance limitations for pairs-construction based methods.

Fortunately, although the number of point clouds data is limited, point clouds typically appear in pairs with images, in which the calibration and time compensation are generally completed. A straightforward approach to achieve 3D open-world understanding involves initially applying 2D open-world models for labeling on images, followed by 3D-2D projecting to derive the corresponding semantic categories (refer 4.4 for details). However, as shown in Figure 1 (b), the projection between images and point clouds is inaccurate (due to factors such as vehicle motion bumps, calibration and compensation errors, etc.), causing numerous false positives and omissions in the projected 3D semantics. Given the spatially paired point clouds and images, along with feature-aligned images and text in visual language models, images can serve as a bridge in a unified learning framework, easing the challenge of aligning text with point clouds. To implement the unified open-world 3D understanding framework with limited 3D data, the following challenges must be addressed: (i) co-embedding the point cloud features with pre-aligned images and text in a shared space, despite limited data availability, (ii) correcting projection misalignments between point clouds and images, and (iii) stably training the unified multi-modal framework to achieve the excellent performance.

Specifically, we begin by constructing the image regional semantic labels by 2D foundation models to supervise the new categories during training. UniPLV integrates a point

*Corresponding Author

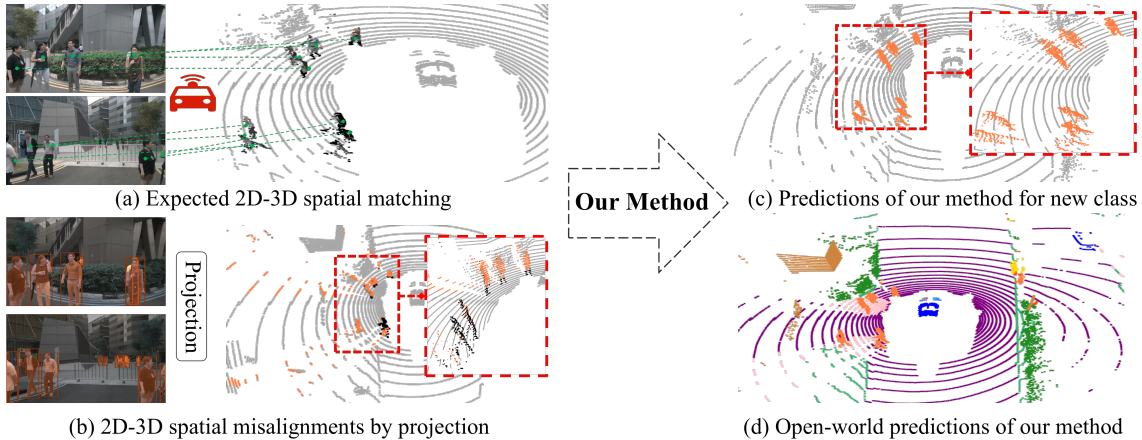


Figure 1. The matching example of 2D images and 3D point clouds. (a): Expected matching between images and point clouds. (b): Image semantic labels are assigned to the corresponding point clouds by projection, which has many false positive mismatched points. (c): The semantic predictions of new classes without any manual annotations by our method. (d): Semantic prediction of our method for all points of an input point cloud.

clouds understanding network and a pre-aligned visual language model, where the image branch is the bridge we need to use. With the image-text alignment and the spatial projection between point clouds and image, we design the classification logits distillation and the feature distillation between image and point clouds modalities to co-embed point clouds with text and images in the same feature space. We further propose a vision-point matching (VPM) learning module to refine point-pixel matching and correct point clouds text alignment. To address the challenges of novel classes being buried as long-tail categories and the gradient bias in multi-modal training, we introduce a two-stage training procedure and four task-specific weighted losses, including image-text alignment, point-text alignment, pixel-point matching, and distillation losses. The training begins with an initial stage focused on independently training the image branch for half of the total iterations, followed by a joint training stage for both image and point clouds branches with distinct loss weights to effectively balance their contributions. Simply providing text descriptions and point clouds, our method could obtain 3D semantic understanding of point clouds during inference.

In summary, our contributions can be summarized into four-fold:

- We propose a unified multi-modal contrastive learning framework for open world 3D scene understanding without constructing point clouds text pairs.
- We propose logit distillation, feature distillation, and vision-point matching modules to co-embed three modalities in a shared feature space.
- We propose a two-stage optimization strategy and four task-specific weighted losses to ensure the stable and efficient multi-modal training.
- Our proposed method achieves the state-of-the-art perfor-

mance for two open world tasks conducted on nuScenes, and is further evaluated on two additional competitive outdoor datasets, Waymo and SemanticKITTI.

2. Related works

3D Semantic Segmentation. Semantic segmentation for LIDAR point clouds can be categorized into three categories based on the form of modeling points, *i.e.*, view-based, point-based, and voxel-based methods. View-based methods convert 3D point clouds to the range view [16, 17, 20] or the bird-eye[41] view to extract 2D features with loss of 3D geometric characteristics. Point-based methods [14, 23, 30, 31, 43] directly use points as inputs to the model and design algorithms to assemble contexts. Voxel-based approaches [6, 9, 10, 42, 45] subdivide the point cloud space into numerous voxel grids and process these voxel features using sparse convolution techniques to improve effectiveness. This paper uses MinkUNet [6], SparseUnet32 [9], and PTV3 [31] as the backbone network to verify the scalability and lightweight of the proposed framework, respectively.

Open-Vocabulary 2D Scene Understanding. The recent advances of large visual language models have expanded the ability to understand 2D open-world scenes. There are two main directions: CLIP-based and Grounding. CLIP-based methods usually replace the linear projection feature with the CLIP feature and use CLIP for feature alignment, such as GLEE[29], DetCLIP series[35–37], RegionCLIP[44], OWL-ViT[21]. The input of Grounding tasks is a picture and a corresponding description. Grounding tasks output object boxes at the corresponding positions in the image based on different descriptions [15, 18, 26, 39]. Given the success of 2D open world understanding, we select GLEE[29] and Grounding DINO[18, 26] as our 2D

open set region label generators, respectively.

Open-Vocabulary 3D Scene Understanding. Open-world 3D scene understanding aims to recognize objects that are not annotated. Early methods [3, 5, 19, 32] mainly achieve open-world understanding through feature differentiation or generation approaches. With the success of visual-language (VL) models, such as CLIP [24], numerous efforts [4, 12, 22, 28, 40] have emerged to transfer the VL knowledge to 3D scene understanding. Clip2Scene [4] utilizes frozen CLIP to obtain semantic labels of images, which are subsequently projected to guide a point cloud semantic segmentation. OpenMask3D [28] employs a 3D instance segmentation network to create 3D masks, which are projected to obtain 2D masks. These 2D masks are then fed into CLIP to extract visual features and match them with textual features, ultimately obtaining 3D semantics. Since CLIP is trained based on full image and text alignments, its capability to comprehend specific regions is limited. OpenScene [22] facilitates point cloud and text alignment by projecting the prediction results from a frozen 2D vision model and employing distillation between image and point clouds features. However, OpenScene requires resource-intensive feature extraction and fusion, and the image backbone is fixed during training, making it unable to be easily expanded to more advanced 3D networks and 3D scenes. Region-PLC [34] and PLA [7] achieve open world 3D scene understanding by constructing a large number of point clouds text pairs to train point clouds and text alignment. In this work, we propose a unified multimodal framework for open world 3D scene understanding, which is lightweight and scalable, while not requiring the production of additional point clouds text pairs.

3. Method

3.1. Overview

We present UniPLV, a new approach for open-vocabulary 3D scene understanding. UniPLV can identify novel categories without manual annotation, while also preserving the performance of base categories annotated manually. To be formalized, given a dataset of 3D point clouds containing categories $(\mathcal{C}_b \cup \mathcal{C}_n)$, s.t. $\mathcal{C}_b \cap \mathcal{C}_n = \emptyset$. The method only accesses manual annotation of base categories \mathcal{C}_b during training, but it can provide labels for both the base categories \mathcal{C}_b and the novel categories \mathcal{C}_n during inference.

In contrast to previous works that achieved open vocabulary understanding by constructing 3D points-text pairs, our work transfers the open vocabulary capability from 2D to 3D by utilizing image regional semantic labels from 2D foundation models without any additional data processing (Sec.3.2). With the 2D-3D spatial mapping and pre-aligned images and texts, we design a multi-modal unified training framework that uses images as a bridge to embed point

cloud features into the shared feature space of images and text. In Sec.3.3, we introduce main components of the proposed framework, the transformation of data flow, two knowledge distillation modules, and a vision-point matching module. Four task-specific optimization objectives are discussed in Sec.3.4. We introduce a multi-modal and multi-task training strategy to ensure stable and efficient training of point cloud and image branches (Sec.3.5). During inference, this framework only requires point clouds and class descriptions as input to compute feature similarity, selecting the most similar class as the semantic prediction for each point (Sec.3.6).

3.2. Image Data Processing

Analysis. Due to the more accessible and larger image-text pairing datasets, recent 2D open-world methods have made significant progress by aligning images and text through contrastive learning. Despite the scarcity of point clouds and the complexity of constructing point clouds-text pairs, point clouds and images are usually captured together and spatially aligned through calibration, which inspires us to use images as a bridge to align point clouds and text into a unified feature space. Considering that image-level alignment data generated by large-scale visual language models such as CLIP could not satisfy the needs of point-level scene understanding, we utilize 2D foundation models to obtain pixel-level correspondences between text semantics and image regions. We would like to emphasize that, despite the predicted image region semantics being noisy and presenting numerous misalignments when transferred to the 3D scene through projection, as illustrated in Figure 1, our designed multi-modal unified training framework, employing images as a bridge, can accurately identify and locate point clouds for given categories.

Region-Text Generation. Intuitively, we extract instance and pixel semantics from 2D vision-language foundation models. Specifically, given a set of images $\mathbf{I} = \{\mathbf{I}_n | n = 1, \dots, N\}$ and the category list $\{t_c\}_{c=1}^C$ as input, where t_c represents for the k-th category name, e.g., $T = [$ "car", "pedestrian", "bicycle", ... , "motorcycle"], the data pipeline output the bounding boxes $\hat{\mathbf{b}}$, instance mask $\hat{\mathbf{m}}$ and the category name $\hat{\mathbf{t}}$ for each image. We use GLEE [29] for instance mask and bounding box generation, which has been trained on large-scale datasets with high accuracy and generalization. We combine Grounding DINO [18] and SAM2 [25] to generate another set of instance labels. Bounding boxes were generated via the Grounding DINO, and each box was further segmented using SAM2 to produce instance masks. We obtain the region-pixel-text pairs $(\hat{\mathbf{b}}, \hat{\mathbf{m}}, \hat{\mathbf{t}})$, as well as the point clouds spatio-temporally aligned to the images, to train the designed 3D scene understanding network transferred from regional image-text alignment. 2D semantic labels for the experimental results

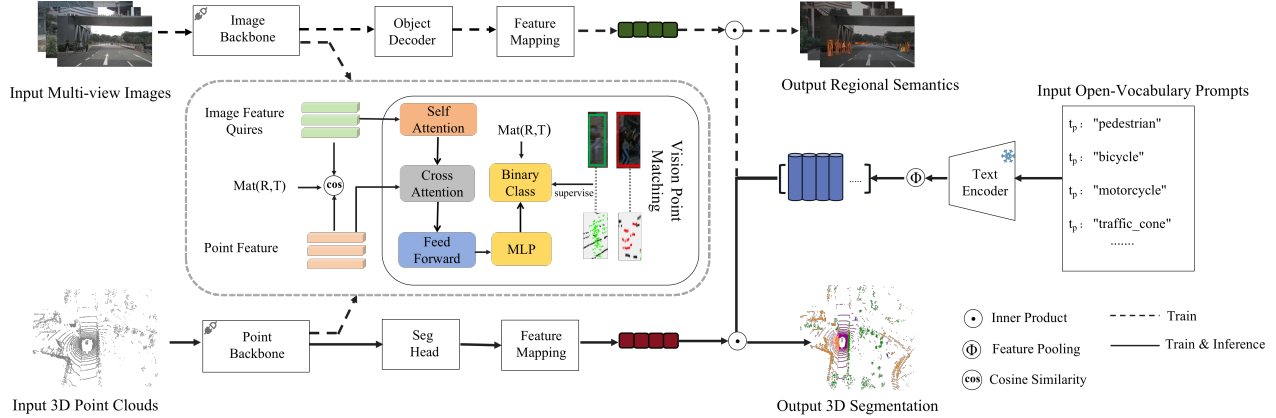


Figure 2. Overview of our proposed multi-modal unified learning framework, Uni-PLV. We utilize 2D foundation models to construct the regional semantic labels for images, which serve as the new classes supervisory signals. We input all category names as text prompts into the text encoder to get text embeddings. Given the spatial temporal aligned point clouds and multi-view images, we extract features using both 2D and 3D branches and compute similarities with text embeddings to obtain semantic categories for pixels and points. We distill classification logits and features of images onto the point cloud to shorten the feature distance of three modalities. Images and point clouds features are also input to vision-point matching module to predict whether points and pixels match. Simply providing text descriptions and point clouds, this framework could obtain 3D semantic understanding during inference.

in this paper are from GLEE, and related experiments on Grounding DINO with SAM2 can be found in the supporting materials.

3.3. Multi-Modal Alignment

3.3.1 Model Framework

The proposed UniPLV consists of a frozen text encoder, image encoder-decoder, and point cloud segmentation branch, as illustrated in Figure 2. We input all category names as text prompts into the text encoder. We follow GLEE to apply global average pooling along the sequence dimension to get text embeddings emb_t . To support open-world understanding, we replace the classifier of image decoder and 3D segment head by the similarity measurement between perception features with text embeddings. Classification logits of 2D L_I and 3D L_P are computed as follows:

$$L_I = \phi(F_I(I) \cdot W_{i2t}, emb_t), \quad (1)$$

$$L_P = \phi(F_p(P) \cdot W_{p2t}, emb_t), \quad (2)$$

where ϕ is the dot product, $\{W_{i2t}, W_{p2t}\}$ are the mapping weights from image and point cloud to text feature dimension, $\{F_I, F_p\}$ are feature extractors for image branch and point cloud branch.

At each iteration e of the training, we have a set of images $\{\mathbf{I}_e^k \in \mathbb{R}^{H \times W \times 3} | k = 1, \dots, K\}$ captured by K cameras, where H and W are image dimensions. We also have the corresponding point cloud $\mathbf{P}_e \in \mathbb{R}^{N_e \times 3}$ with the mapping matrix Γ_{lc} from LiDAR coordinate to image coordinate. Given the category list $\{t_c\}_{c=1}^C$, images $\{\mathbf{I}_e^k\}$ and the point cloud \mathbf{P}_e as input, UniPLV could fine-tune the segmentation and detection of the image with the constructed

regional image-text pairs $\langle \hat{\mathbf{b}}, \hat{\mathbf{m}}, \hat{\mathbf{t}} \rangle$, and provide the segmentation results of the point cloud corresponding to the given category list. The ultimate optimization goal of this framework is to embed point cloud features and image-text features into a unified feature space through multi-modal joint training, enabling the alignment of point cloud and text for open-world 3D scene understanding.

For the image and text branches, we load the second stage model of GLEE as pre-training weights to strengthen the alignment of text and images. During training, we fine-tune the image model using data constructed by 2D foundation models, exploiting the model’s learning capability to eliminate noise from raw labels without additional processing. During iterative training, the model inherently engages in feature clustering that identifies and learns the common attributes of the given category. This mechanism helps in filtering out noise introduced by false positives, thereby contributing to the effective cleaning of pseudo-labels.

3.3.2 Vision-Point Knowledge Distillation

To construct the framework in which image acts as a bridge for the joint embedding of point cloud features and pre-aligned image-text pairs into a unified feature space, we introduce two distillation modules: logit distillation and feature distillation.

Logit Distillation. The semantic classification logits L_I of image pixels are obtained through similarity measurement between the image feature and all given categories text embeddings as eq.1. Similarly, the semantic classification logits L_P of point clouds are also obtained by calculating similarity with text as eq.2. We design the logit distilla-

tion $\mathcal{L}_{distill_L}$ supervising the point cloud classification logits L_P with novel class semantics S_{C_n} predicted by the image branch as follows:

$$S_{C_n} = \sigma(L_I) \rightarrow Proj(\Gamma_{Ic}, \mathbf{P}), \quad (3)$$

$$\mathcal{L}_{distill_L} = \mathcal{L}_{CE}(L_P, S_{C_n} \cup Ig_{C_b}) + \mathcal{L}_{Dice}(L_P, S_{C_n} \cup Ig_{C_b}), \quad (4)$$

where σ is the sigmoid function and S_{C_n} are the category labels used to supervise the 3D segmentation of new classes, which obtained by mapping the predictions of the image through projection matrix Γ_{Ic} ; Ig_{C_b} are masked labels of base class points; \mathcal{L}_{CE} and \mathcal{L}_{Dice} denote the Cross-Entropy loss and Dice loss.

Feature Distillation. The alignment between images and text has been pretrained using large-scale data. To bridge the gap between point clouds and semantic text, we further distill the features of point clouds using image features. We exclusively distill 2D-3D paired points that simultaneously align in terms of spatial projection mapping and corresponding semantics. Feature distillation $\mathcal{L}_{distill_F}$ is performed based on similarity measurement as follows:

$$\mathcal{L}_{distill_F} = 1 - CoDist(F_I(I_m) \cdot W_{i2t}, F_P(P_m) \cdot W_{p2t}) \quad (5)$$

Where $CoDist(\cdot)$ represents the cosine similarity function, I_m and P_m are 2D-3D pairings that align spatially and semantically.

3.3.3 Vision-Point Matching Learning

We introduce the vision-point matching (VPM) module to further learn fine-grained alignment between images and point clouds. It is a binary classification task that requires the model to predict whether the pixel-point pairs from the projection are positive (matched) or negative (unmatched). VPM mainly includes an attention encoder module and a binary classifier. Given the paring image features and the point cloud features, the image feature acts as the query vector Q_I , while the point cloud features serve as the key K_P and value vectors V_P . Self-attention is applied to the image features obtaining image attention feature Q_{attenI} . Followed cross-attention between the Q_{attenI} and point cloud features as:

$$\xi_i = \sigma\left(\frac{Q_{attenI}K_P}{\sqrt{d^{\xi}}}\right)V_P, \quad (6)$$

where ξ_i is the obtained cross-attention features; σ denotes softmax and d^{ξ} is the dimension of each ξ . The attention encoder can be formulated as:

$$ENCODE_{vpm} = \mathcal{FFN}(\text{cat}(\xi_1, \dots, \xi_h)), \quad (7)$$

where \mathcal{FFN} is a feed-forward network, which consists of MLPs and activations; After the VPM encoder gets the attention map $G_{attenIP}$ of the projection paring points and

pixels, the matching probability is obtained by a binary classifier:

$$\hat{f}_{map} = MLP(G_{attenIP}), \quad f \in R^{r \times 2}, \quad (8)$$

where r is the number of points and pixels that matched after projection; MLP denotes the multilayer perceptron for binary classification. The VPM module uses base and novel classes of paring pixels and points for supervision during training.

3.4. Optimization Objective

We jointly train the alignment of image pixels and 3D points with text to achieve 3D open-world scene understanding. There are four task-specific losses of our UniPLV: images-text alignment, points-text alignment, pixel-point matching, as well as logits and feature distillation loss. The final overall loss is obtained by combining the above four types of losses with balancing weights as follows:

$$\mathcal{L} = \beta\mathcal{L}_{image} + \delta\mathcal{L}_{point} + \gamma\mathcal{L}_{distillation} + \gamma\mathcal{L}_{VPM} \quad (9)$$

where β, δ, γ denote the weights of losses; \mathcal{L}_{image} denotes the image-text alignment loss, which aims to predict boxes and semantic masks for images; \mathcal{L}_{point} is the points-text alignment loss optimizing the segmentation of both base and new classes; $\mathcal{L}_{distillation}$ denotes the combination of logit distillation loss $\mathcal{L}_{distill_L}$ and feature distillation loss $\mathcal{L}_{distill_F}$; \mathcal{L}_{VPM} represent the vision-point matching(VPM) loss to minimize projection errors between 3D points and 2D pixels. The VPM loss is then defined as:

$$\mathcal{L}_{VPM} = BCE(\hat{f}_{map}, \mathbf{M}_{align}), \quad \mathbf{M}_{align} = \begin{cases} 1 & \text{if } L_P == L_I \rightarrow Proj(\Gamma_{Ic}, \mathbf{P}), \\ 0 & \text{otherwise.} \end{cases} \quad (10)$$

where BCE denotes the Binary Cross-Entropy loss. The elements in \hat{f}_{map} , represent the matching labels between points and pixels, which are 1 if matched and 0 otherwise. The final loss is obtained by combining the above four types of losses with balancing weights. The specific formal expression of each loss can refer to the supporting materials.

3.5. Multi-Modal and Multi-Task Training

We present a two-stage multi-task training strategy designed to train the multi-modal framework UniPLV.

Stage 1: Independent image branch training. The training begins with a preliminary phase where we train the image branch independently, utilizing half of the total iteration steps to ensure a stable and robust foundation. We implement gradient clipping exclusively during the image branch training to prevent exploding gradients and stabilize the training dynamics.

Stage 2: Unified multimodal training. The second stage involves joint training of both the image and point cloud branches, employing distinct loss weights to balance their contributions effectively. Throughout the training process, we consistently utilize the AdamW optimizer, chosen for its adaptive learning capabilities and improved convergence properties. The optimizer parameters, specifically the learning rate and weight decay, are set differently for the image and point cloud branch depending on the backbone of each branch. This strategic differentiation in optimizer settings ensures that both branches are training according to their specific network structures and data characteristics, ultimately leading to superior performance in multi-modal training tasks.

Benefits of the two-stage training schemes, particularly for new classes, are detailed in the experimental section.

3.6. Inference

The inference process is depicted in the Figure 2. During inference, we can encode any arbitrary open-vocabulary categories as text queries and compute their similarity with the observed 3D points. Specifically, we associate each point with the category having highest computed cosine similarity. Our method does not require processing images during inference, since we have distilled the image-text alignment to the point cloud.

4. Experiment

4.1. Basic Setups

Datasets. We evaluate our approach on three competitive outdoor datasets: nuScenes [2], SemanticKITTI [1], and Waymo [27]. Following RegionPLC [34], we evaluate the open-world understanding capabilities on two tasks: base-annotated open world (i.e. part of categories annotated) and annotation-free open world (i.e. no category annotated). For the base-annotated open-world task, we split the categories of the mentioned three datasets into base and novel classes, respectively. As for nuScenes, we follow the category partition of RegionPLC, disregarding the ambiguous category "other_flat" and randomly divide the remaining 15 classes into B12/N3 (i.e. 12 base and 3 novel categories) and B10/N5. We randomly split the category into B15/N2 for Waymo and B17/N2 for SemanticKITTI. Please refer Suppl. for more details.

Implementation Details and Evaluation Metrics. We build the text and image branch upon GLEE [29], adopting CLIP [24] text encoder to process text descriptions and MaskDINO [13] as image encoder-decoder. We utilize the MinkUNet [6], SparseUnet32 [9], and PTv3 [31] as point cloud backbone. We use the ADAM optimizer with a batch size of 32 on 16 NVIDIA A800 GPUs. We use the mean intersection-over-union (mIoU) and harmonic mean IoU

(hIoU) as the evaluation indicators. Further training details can be found in the supplementary materials.

4.2. Quantitative Results

4.2.1 Base-Annotated Open-World

Table 1 shows major comparison methods, among which RegionPLC is the current SOTA method. Since the results of public methods are mainly on nuScenes benchmark, we mainly compare with other methods on the nuScenes dataset. In SemanticKITTI and Waymo datasets, only the gap with full supervision and visual analysis are presented. **nuScenes results.** For a fair and detailed comparison, we present the results of three point cloud segmentation backbones in Table 1. Using the same point cloud backbone SparseUnet32 as RegionPLC, our method largely lifts the mIoU of unseen categories by 6.2% ~21.8% among various partitions on nuScenes without constructing any point-text pairs. When utilizing the higher-performance backbone network, PTv3, our approach achieves a mIoU gain of 10.5% ~27.7% for the new classes compared to Region-PLC. Even with a lower performance backbone, MinkUNet, our method still outperforms RegionPLC by 0.3% ~20.7% for new classes. While achieving significant improvements in the new classes, we can keep the mIOU of the base classes fluctuating within 0.3% ~3% compared to fully supervised performance. Comparing the 3DGenZ and 3DTZSL, which omit language alignment, our method even obtains 60.1% ~65.9% gain on mIoU of new classes. The results for different backbone substitutability demonstrate the adaptability and integrability of our method.

SemanticKITTI and Waymo results. As shown in Tab 2, partition B15/N2 on Waymo shows only a 6.4% difference in new classes performance compared to the full supervision, which demonstrates the robustness and practicality of our approach in open-world 3D scene understanding. On the SemanticKITTI dataset, the performance of B17/N2 partition differs from fully supervised classes by 15.1%. It should be pointed out that the SemanticKITTI dataset only has forward-looking image, and we only capture point clouds at a forward angle of 120° for experimentation, which leads to a large performance gap with full supervision. The results on these two datasets demonstrate the broad applicability of our proposed method in different scenarios.

4.2.2 Annotation-Free Open-World Segmentation.

We evaluate the annotation-free capability of our method on the nuScenes validation set, which consists of 16 categories. We freeze the image branch of the proposed UniPLV and load the pre-trained weights from GLEE. Without any 2D or 3D annotations, we have successfully transferred 2D open-world capabilities to 3D through distillation and matching

	Methods	B12/N3			B10/N5		
		hIoU	mIoU _B	mIoU _N	hIoU	mIoU _B	mIoU _N
Full supervision	SparseUnet32 [9]	75.2	76.6	73.8	75.7	76.6	74.8
	MinkUNet [6]	70.9	74.6	67.7	72.3	74.8	70.0
	PTv3 [31]	77.2	79.9	74.8	77.6	78.20	77.1
Open-World	3DGenZ [19]	1.6	53.3	0.8	1.9	44.6	1
	3DTZSL [5]	1.2	21.0	0.6	6.4	17.1	3.9
	Ovseg-3D [12]	0.6	74.4	0.3	0	71.5	0
	PLA [7]	47.7	73.4	35.4	24.3	73.1	14.5
	RegionPLC [34] (SparseUnet32)	64.4	75.8	56.0	49.0	75.8	36.3
	UniPLV(SparseUnet32)	68.3	75.9	62.2	65.3	75.9	57.3
	UniPLV(MinkUNet)	64.1	74.3	56.3	64.5	74.2	57.0
	UniPLV(PTv3)	71.3	76.9	66.5	69.6	76.3	64.0

Table 1. **Open-world 3D semantic segmentation comparisons on nuScenes Benchmark.** Full supervision: Both base and new classes are gt labels. Open-world: Best open-world results are presented in bold.

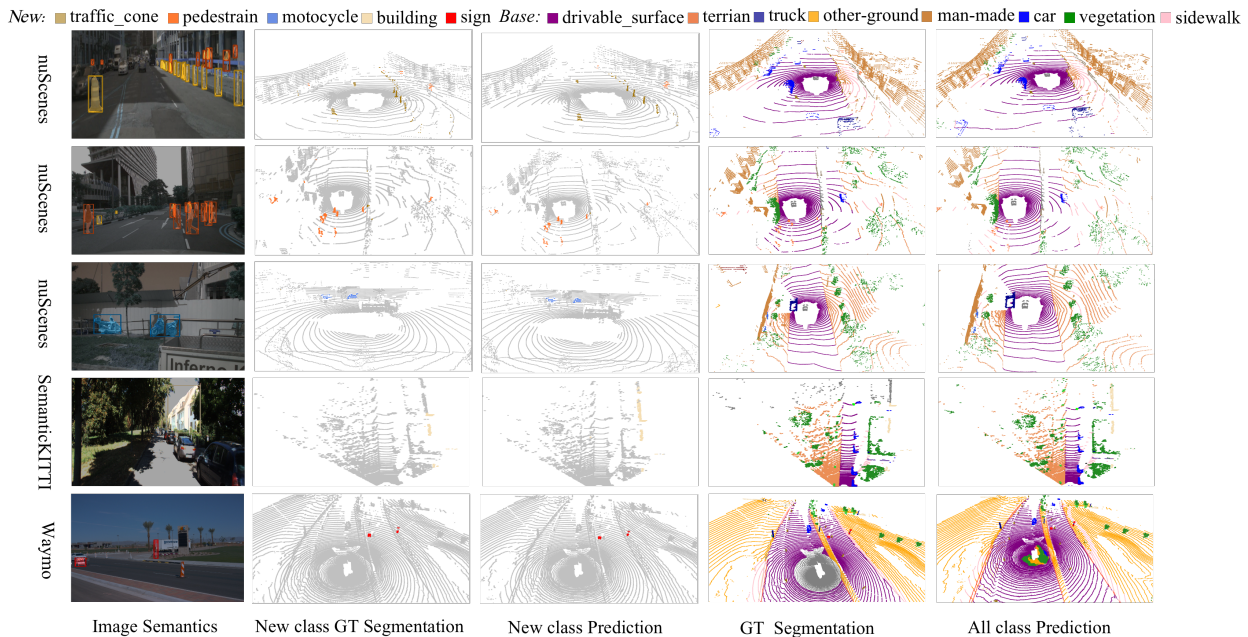


Figure 3. **Qualitative results of the base-annotated task.**

Datasets	Methods	mIoU _B	mIoU _N
Waymo [27]	Full Supervision(PTv3)	74.3	81.8
	UniPLV(PTv3)	74.0	75.4
SemanticKITTI [1]	Full Supervision (PTv3)	57.7	77.4
	UniPLV(PTv3)	57.4	62.3

Table 2. Open-world evaluation on the SemanticKITTI and Waymo datasets.

learning. As shown in Table 3, we compare our approach to the most closely related work on zero-shot 3D semantic segmentation: CLIP2Scene [4], OpenScene [22], and MSeg [11] Voting. UniPLV achieves better performance than the above three methods. UniPLV outperforms CLIP2Scene with 36.1%, OpenScene with 14.8%, and MSeg Voting with 25.9%, respectively.

Methods	nuScenes
CLIP2Scene [4]	20.8
OpenScenes [22]	42.1
MSeg[11] Voting	31.0
UniPLV	56.9

Table 3. Comparison for annotation-free task on nuScenes.

Transfer Pipeline	mIoU _N
2D-3D projection	28.6
UniPLV	66.5

Table 4. Comparison with projected-only approach.

One-Stage	Two-Stage	\mathcal{L}_{logits}	$\mathcal{L}_{distill_N}$	$\mathcal{L}_{distill_F}$	\mathcal{L}_{VPM}	mIoU _B	mIoU _N
✓		✓				73.2	57.3
✓		✓	✓	✓	✓	74.1	58.2
	✓	✓				76.6	60.1
	✓	✓	✓			76.4	62.6
	✓	✓	✓	✓		76.8	65.2
	✓	✓	✓	✓	✓	76.9	66.5

Table 5. Optimization analysis: including ablation study for two stage optimization strategies and various loss functions.

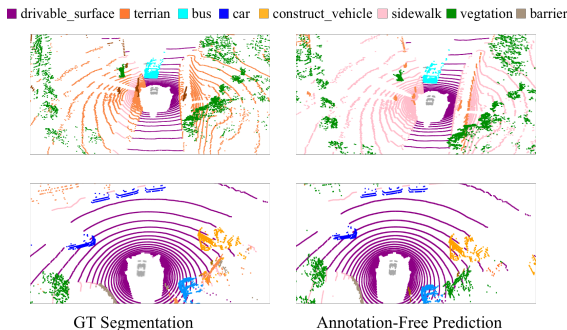


Figure 4. Qualitative results of the annotation-free task.

4.3. Qualitative analysis

We further demonstrate the open-world 3D understanding capabilities of the proposed method through visualization. As shown in Figure 3, our method successfully identifies and locates new categories while ensuring the recognition accuracy of base categories. The object detected by the image can be located by the point cloud network, and some false detections in the image can also be adaptively filtered out by the point cloud network. For some relatively small and distant targets with few points, such as traffic cones and distant pedestrians, our method still locates and identifies them. Figure 4 demonstrates the open-world 3D scene understanding ability of our method on annotation-free task. The overall point cloud clustering groups identified by our method are basically consistent with the GT. Background categories, such as plants, drivable areas, sidewalks, and long-tail categories, such as construction vehicles and buses, have been successfully identified. Classes that are easily confused conceptually, such as terrain and sidewalk, may present cross-misrecognition due to the fact that large text models learn a wide range of vocabulary, resulting in blurred boundaries between similar vocabularies.

4.4. Ablation Studies

The ablation experiments are all conducted on nuScenes based on the category partition B12/N3. **Multi-Modal Learning Framework.** To verify the contrastive learning ability of the proposed framework, we directly project point clouds into images to get 2D pixel semantics predicted by 2D foundation models. As shown in Table 4, our proposed framework outperforms

the projection-only approach by 37.9% of mIoU on new classes. This experiment shows that the proposed framework can align the three modes well with limited point clouds data.

Alignment and Optimization. Table 5 presents impact of different modules, corresponding optimization losses, and the two-stage training procedure. In comparative experiments between one-stage and two-stage training, two stage-training yields an improvement of 2.8% ~ 8.3% for both base and new classes. Based on the loss \mathcal{L}_{logits} , adding an independent distillation $\mathcal{L}_{distill_N}$ for the new class resulted in a 2.5% increase. The feature distillation loss $\mathcal{L}_{distill_F}$ from pixels to points results in a 2.6% improvement. The vision-point matching learning loss \mathcal{L}_{VPM} brings 1.3% mIoU gains in the new classes. The experimental results demonstrate the effectiveness of our designed 2D to 3D knowledge transfer alignment strategy and provide a valuable reference for multi-modal fusion tasks involving point clouds and images.

5. Conclusion and Future work

Conclusion. We present a unified multi-modal learning framework, termed UniPLV, for open world 3D scene understanding that does not require point cloud text pairs. Leveraging image as a bridge, we propose logits distillation, feature distillation, and modal matching modules. We further introduce four task-specific losses and a two-stage training procedure for stably multi-modal learning. Our method significantly outperforms SOTA methods on nuScenes. Besides, experimental results on different 3D backbones as well as on Waymo and Semantickitti datasets demonstrate the scalability and lightweight of our method.

Future work. There are some works waiting for improvement and solution in the future. Our proposed framework has been validated exclusively on outdoor datasets. In the future, we aim to extend this validation to indoor datasets, e.g. ScanNet, where the projection parameters between 2D and 3D are more accurate. We will improve and quantify the image branch in the future, so that the proposed framework can achieve both 2D and 3D open-world scene understanding tasks simultaneously. The point cloud branch can also be replaced by an occupancy prediction network to extend the open world application.

References

- [1] Jens Behley, Martin Garbade, Andres Milioto, Jan Quenzel, Sven Behnke, Cyrill Stachniss, and Jurgen Gall. Semantickitti: A dataset for semantic scene understanding of lidar sequences. In *Proceedings of the IEEE/CVF international conference on computer vision*, pages 9297–9307, 2019. 6, 7
- [2] Holger Caesar, Varun Bankiti, Alex H Lang, Sourabh Vora, Venice Erin Liong, Qiang Xu, Anush Krishnan, Yu Pan, Giancarlo Baldan, and Oscar Beijbom. nuscenes: A multi-modal dataset for autonomous driving. In *Proceedings of the IEEE/CVF conference on computer vision and pattern recognition*, pages 11621–11631, 2020. 6
- [3] Jun Cen, Peng Yun, Shiwei Zhang, Junhao Cai, Di Luan, Mingqian Tang, Ming Liu, and Michael Yu Wang. Open-world semantic segmentation for lidar point clouds. In *European Conference on Computer Vision*, pages 318–334. Springer, 2022. 3
- [4] Runnan Chen, Youquan Liu, Lingdong Kong, Xinge Zhu, Yuexin Ma, Yikang Li, Yuenan Hou, Yu Qiao, and Wenping Wang. Clip2scene: Towards label-efficient 3d scene understanding by clip. In *Proceedings of the IEEE/CVF Conference on Computer Vision and Pattern Recognition*, pages 7020–7030, 2023. 3, 7
- [5] Ali Cheraghian, Shafin Rahman, Dylan Campbell, and Lars Petersson. Transductive zero-shot learning for 3d point cloud classification. In *Proceedings of the IEEE/CVF winter conference on applications of computer vision*, pages 923–933, 2020. 3, 7
- [6] Christopher Choy, JunYoung Gwak, and Silvio Savarese. 4d spatio-temporal convnets: Minkowski convolutional neural networks. In *Proceedings of the IEEE/CVF conference on computer vision and pattern recognition*, pages 3075–3084, 2019. 2, 6, 7
- [7] Runyu Ding, Jihan Yang, Chuhui Xue, Wenqing Zhang, Song Bai, and Xiaojuan Qi. Pla: Language-driven open-vocabulary 3d scene understanding. In *Proceedings of the IEEE/CVF conference on computer vision and pattern recognition*, pages 7010–7019, 2023. 1, 3, 7
- [8] Runyu Ding, Jihan Yang, Chuhui Xue, Wenqing Zhang, Song Bai, and Xiaojuan Qi. Lowis3d: Language-driven open-world instance-level 3d scene understanding. *IEEE Transactions on Pattern Analysis and Machine Intelligence*, 2024. 1
- [9] Benjamin Graham, Martin Engelcke, and Laurens Van Der Maaten. 3d semantic segmentation with submanifold sparse convolutional networks. In *Proceedings of the IEEE conference on computer vision and pattern recognition*, pages 9224–9232, 2018. 2, 6, 7
- [10] Xin Lai, Yukang Chen, Fanbin Lu, Jianhui Liu, and Jiaya Jia. Spherical transformer for lidar-based 3d recognition. In *Proceedings of the IEEE/CVF Conference on Computer Vision and Pattern Recognition*, pages 17545–17555, 2023. 2
- [11] John Lambert, Zhuang Liu, Ozan Sener, James Hays, and Vladlen Koltun. Mseg: A composite dataset for multi-domain semantic segmentation. In *Proceedings of the IEEE/CVF conference on computer vision and pattern recognition*, pages 2879–2888, 2020. 7
- [12] Boyi Li, Kilian Q Weinberger, Serge Belongie, Vladlen Koltun, and René Ranftl. Language-driven semantic segmentation. *arXiv preprint arXiv:2201.03546*, 2022. 3, 7
- [13] Feng Li, Hao Zhang, Huaizhe Xu, Shilong Liu, Lei Zhang, Lionel M Ni, and Heung-Yeung Shum. Mask dino: Towards a unified transformer-based framework for object detection and segmentation. In *Proceedings of the IEEE/CVF Conference on Computer Vision and Pattern Recognition*, pages 3041–3050, 2023. 6
- [14] Hao Li, Zehan Zhang, Xian Zhao, Yulong Wang, Yuxi Shen, Shiliang Pu, and Hui Mao. Enhancing multi-modal features using local self-attention for 3d object detection. In *European Conference on Computer Vision*, pages 532–549. Springer, 2022. 2
- [15] Liunian Harold Li, Pengchuan Zhang, Haotian Zhang, Jianwei Yang, Chunyuan Li, Yiwu Zhong, Lijuan Wang, Lu Yuan, Lei Zhang, Jenq-Neng Hwang, et al. Grounded language-image pre-training. In *Proceedings of the IEEE/CVF Conference on Computer Vision and Pattern Recognition*, pages 10965–10975, 2022. 2
- [16] Zhidong Liang, Ming Zhang, Zehan Zhang, Xian Zhao, and Shiliang Pu. Rangercnn: Towards fast and accurate 3d object detection with range image representation. *arXiv preprint arXiv:2009.00206*, 2020. 2
- [17] Zhidong Liang, Zehan Zhang, Ming Zhang, Xian Zhao, and Shiliang Pu. Rangeioudet: Range image based real-time 3d object detector optimized by intersection over union. In *Proceedings of the IEEE/CVF Conference on Computer Vision and Pattern Recognition*, pages 7140–7149, 2021. 2
- [18] Shilong Liu, Zhaoyang Zeng, Tianhe Ren, Feng Li, Hao Zhang, Jie Yang, Qing Jiang, Chunyuan Li, Jianwei Yang, Hang Su, et al. Grounding dino: Marrying dino with grounded pre-training for open-set object detection. *arXiv preprint arXiv:2303.05499*, 2023. 2, 3
- [19] Björn Michele, Alexandre Boulch, Gilles Puy, Maxime Bucher, and Renaud Marlet. Generative zero-shot learning for semantic segmentation of 3d point clouds. In *2021 International Conference on 3D Vision (3DV)*, pages 992–1002. IEEE, 2021. 3, 7
- [20] Andres Milioto, Ignacio Vizzo, Jens Behley, and Cyrill Stachniss. Rangenet++: Fast and accurate lidar semantic segmentation. pages 4213–4220, 2019. 2
- [21] Matthias Minderer, Alexey Gritsenko, and Neil Houlsby. Scaling open-vocabulary object detection. *Advances in Neural Information Processing Systems*, 36, 2024. 2
- [22] Songyou Peng, Kyle Genova, Chiyu Jiang, Andrea Tagliasacchi, Marc Pollefeys, Thomas Funkhouser, et al. Openscene: 3d scene understanding with open vocabularies. In *Proceedings of the IEEE/CVF conference on computer vision and pattern recognition*, pages 815–824, 2023. 1, 3, 7
- [23] Charles Ruizhongtai Qi, Li Yi, Hao Su, and Leonidas J Guibas. Pointnet++: Deep hierarchical feature learning on point sets in a metric space. *Advances in neural information processing systems*, 30, 2017. 2

- [24] Alec Radford, Jong Wook Kim, Chris Hallacy, Aditya Ramesh, Gabriel Goh, Sandhini Agarwal, Girish Sastry, Amanda Askell, Pamela Mishkin, Jack Clark, et al. Learning transferable visual models from natural language supervision. In *International conference on machine learning*, pages 8748–8763. PMLR, 2021. 3, 6
- [25] Nikhila Ravi, Valentin Gabeur, Yuan-Ting Hu, Ronghang Hu, Chaitanya Ryali, Tengyu Ma, Haitham Khedr, Roman Rädle, Chloe Rolland, Laura Gustafson, et al. Sam 2: Segment anything in images and videos. *arXiv preprint arXiv:2408.00714*, 2024. 3
- [26] Tianhe Ren, Qing Jiang, Shilong Liu, Zhaoyang Zeng, Wenlong Liu, Han Gao, Hongjie Huang, Zhengyu Ma, Xiaohe Jiang, Yihao Chen, et al. Grounding dino 1.5: Advance the” edge” of open-set object detection. *arXiv preprint arXiv:2405.10300*, 2024. 2
- [27] Pei Sun, Henrik Kretschmar, Xerxes Dotiwalla, Aurelien Chouard, Vijaysai Patnaik, Paul Tsui, James Guo, Yin Zhou, Yuning Chai, Benjamin Caine, et al. Scalability in perception for autonomous driving: Waymo open dataset. In *Proceedings of the IEEE/CVF conference on computer vision and pattern recognition*, pages 2446–2454, 2020. 6, 7
- [28] Ayça Takmaz, Elisabetta Fedele, Robert W Sumner, Marc Pollefeys, Federico Tombari, and Francis Engelmann. Openmask3d: Open-vocabulary 3d instance segmentation. *arXiv preprint arXiv:2306.13631*, 2023. 3
- [29] Junfeng Wu, Yi Jiang, Qihao Liu, Zehuan Yuan, Xiang Bai, and Song Bai. General object foundation model for images and videos at scale. In *Proceedings of the IEEE/CVF Conference on Computer Vision and Pattern Recognition*, pages 3783–3795, 2024. 2, 3, 6
- [30] Xiaoyang Wu, Yixing Lao, Li Jiang, Xihui Liu, and Hengshuang Zhao. Point transformer v2: Grouped vector attention and partition-based pooling. *Advances in Neural Information Processing Systems*, 35:33330–33342, 2022. 2
- [31] Xiaoyang Wu, Li Jiang, Peng-Shuai Wang, Zhijian Liu, Xihui Liu, Yu Qiao, Wanli Ouyang, Tong He, and Hengshuang Zhao. Point transformer v3: Simpler faster stronger. In *Proceedings of the IEEE/CVF Conference on Computer Vision and Pattern Recognition*, pages 4840–4851, 2024. 2, 6, 7
- [32] Yongqin Xian, Subhabrata Choudhury, Yang He, Bernt Schiele, and Zeynep Akata. Semantic projection network for zero-and few-label semantic segmentation. In *Proceedings of the IEEE/CVF Conference on Computer Vision and Pattern Recognition*, pages 8256–8265, 2019. 3
- [33] Jihan Yang, Runyu Ding, Weipeng Deng, Zhe Wang, and Xiaojuan Qi. Regionplc: Regional point-language contrastive learning for open-world 3d scene understanding. pages 19823–19832, 2024. 1
- [34] Jihan Yang, Runyu Ding, Weipeng Deng, Zhe Wang, and Xiaojuan Qi. Regionplc: Regional point-language contrastive learning for open-world 3d scene understanding. In *Proceedings of the IEEE/CVF Conference on Computer Vision and Pattern Recognition*, pages 19823–19832, 2024. 3, 6, 7
- [35] Lewei Yao, Jianhua Han, Youpeng Wen, Xiaodan Liang, Dan Xu, Wei Zhang, Zhenguo Li, Chunjing Xu, and Hang Xu. Detclip: Dictionary-enriched visual-concept paralleled pre-training for open-world detection. *Advances in Neural Information Processing Systems*, 35:9125–9138, 2022. 2
- [36] Lewei Yao, Jianhua Han, Xiaodan Liang, Dan Xu, Wei Zhang, Zhenguo Li, and Hang Xu. Detclipv2: Scalable open-vocabulary object detection pre-training via word-region alignment. In *Proceedings of the IEEE/CVF Conference on Computer Vision and Pattern Recognition*, pages 23497–23506, 2023.
- [37] Lewei Yao, Renjie Pi, Jianhua Han, Xiaodan Liang, Hang Xu, Wei Zhang, Zhenguo Li, and Dan Xu. Detclipv3: Towards versatile generative open-vocabulary object detection. In *Proceedings of the IEEE/CVF Conference on Computer Vision and Pattern Recognition*, pages 27391–27401, 2024. 2
- [38] Yihan Zeng, Chenhan Jiang, Jiageng Mao, Jianhua Han, Chaoqiang Ye, Qingqiu Huang, Dit-Yan Yeung, Zhen Yang, Xiaodan Liang, and Hang Xu. Clip2: Contrastive language-image-point pretraining from real-world point cloud data. In *Proceedings of the IEEE/CVF conference on computer vision and pattern recognition*, pages 15244–15253, 2023. 1
- [39] Haotian Zhang, Pengchuan Zhang, Xiaowei Hu, Yen-Chun Chen, Liunian Harold Li, Xiyang Dai, Lijuan Wang, Lu Yuan, Jenq-Neng Hwang, and Jianfeng Gao. Glipv2: unifying localization and vl understanding. In *Proceedings of the 36th International Conference on Neural Information Processing Systems*, pages 36067–36080, 2022. 2
- [40] Junbo Zhang, Runpei Dong, and Kaisheng Ma. Clip-fo3d: Learning free open-world 3d scene representations from 2d dense clip. In *Proceedings of the IEEE/CVF International Conference on Computer Vision*, pages 2048–2059, 2023. 1, 3
- [41] Yang Zhang, Zixiang Zhou, Philip David, Xiangyu Yue, Zerong Xi, Boqing Gong, and Hassan Foroosh. Polarnet: An improved grid representation for online lidar point clouds semantic segmentation. In *Proceedings of the IEEE/CVF conference on computer vision and pattern recognition*, pages 9601–9610, 2020. 2
- [42] Zehan Zhang, Yang Ji, Wei Cui, Yulong Wang, Hao Li, Xian Zhao, Duo Li, Sanli Tang, Ming Yang, Wenming Tan, et al. Atf-3d: Semi-supervised 3d object detection with adaptive thresholds filtering based on confidence and distance. *IEEE Robotics and Automation Letters*, 7(4):10573–10580, 2022. 2
- [43] Hengshuang Zhao, Li Jiang, Jiaya Jia, Philip HS Torr, and Vladlen Koltun. Point transformer. In *Proceedings of the IEEE/CVF international conference on computer vision*, pages 16259–16268, 2021. 2
- [44] Yiwu Zhong, Jianwei Yang, Pengchuan Zhang, Chunyuan Li, Noel Codella, Liunian Harold Li, Luwei Zhou, Xiyang Dai, Lu Yuan, Yin Li, et al. Regionclip: Region-based language-image pretraining. In *Proceedings of the IEEE/CVF conference on computer vision and pattern recognition*, pages 16793–16803, 2022. 2
- [45] Hui Zhou, Xinge Zhu, Xiao Song, Yuexin Ma, Zhe Wang, Hongsheng Li, and Dahua Lin. Cylinder3d: An effective 3d framework for driving-scene lidar semantic segmentation. *arXiv preprint arXiv:2008.01550*, 2020. 2